Flow characteristics of spray impingement in PFI injection systems

by

M. R. O. Panão and A. L. N. Moreira [(1)]

Instituto Superior Técnico
Mechanical Engineering Department
Av. Rovisco Pais, 1049-001 Lisboa; Portugal
[(1)]E-Mail: moreira@dem.ist.utl.pt

ABSTRACT

Internal Combustion engines with multi-point, or sequential, fuel injection have a fuel injector for each cylinder, usually located so that they spray right at the intake valve. While in a fully warmed-up engine, fuel droplets vaporize before entering the combustion chamber, at cold start, a significant proportion of the injected gasoline deposits on the intake port and valve surfaces. The result is a deterioration of mixture homogeneity, decreased metering accuracy and increased hydrocarbon emissions. A better control of mixture preparation at cold start conditions can be achieved if the interaction between the gasoline spray and the time-varying liquid film which forms during the period of injection can be accurately predicted. The work reported here considers part of an experimental study performed with that objective in a purposed built experiment considering a simplified geometry.

Droplet characteristics measured with a PDA system in the vicinity of the impact surface, prior and right after the impact, are used to infer about the transient spray-wall interaction mechanisms when a liquid film forms. Conservation laws allow to derive the fractions (α_θ) of mass, momentum and energy from the spray prior to impact that are transferred to/from the liquid film. Most of the inflowing mass deposits within the core of the spray and transfers momentum to the liquid film in the radial direction, influencing the velocity and direction of secondary droplets formed at impingement. The use of α_θ, together with the mass flux ratio of outgoing to inflowing droplets in existing empirical correlations to predict the impingement outcome, is shown to improve prediction of flux ratios, either of number, momentum or energy. These fractions are suggested as a simple way of including the influence of the liquid film in spray/wall interaction and their modelling is the scope of future work.

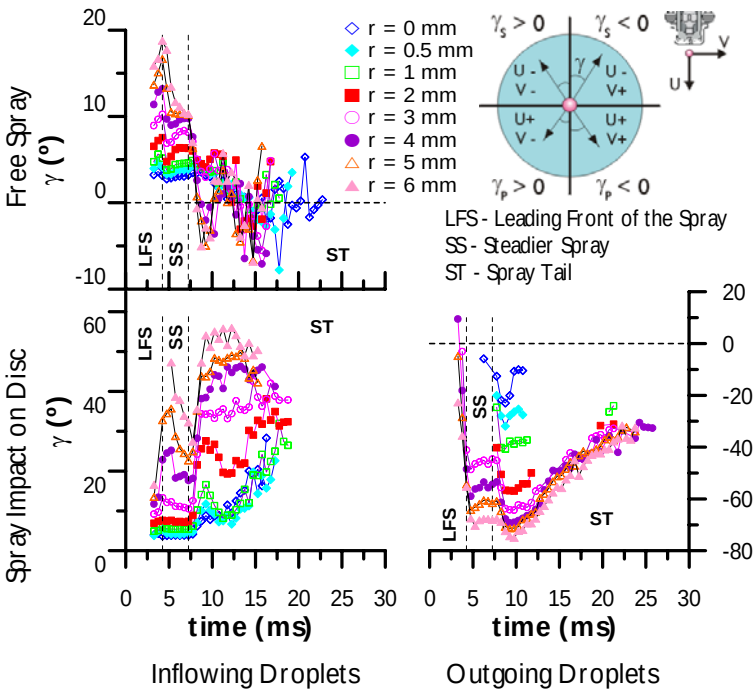

Time variation of the direction of a) droplets in the free spray; b) inflowing droplets of the impacting spray and c) secondary droplets after impact.

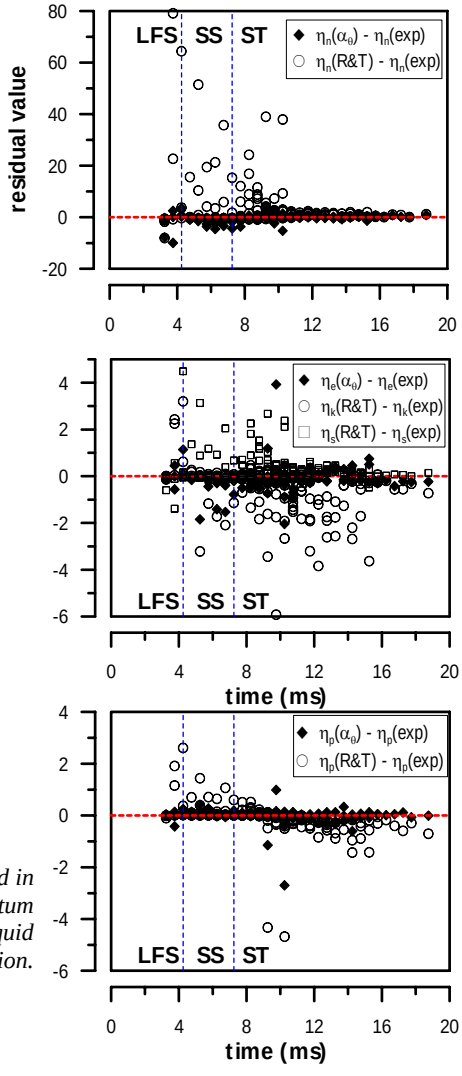

The plots of residuals show the improvement achieved in the models to predict the fractions of mass, momentum and energy of inflowing droplets transferred to the liquid film during injection.

1. INTRODUCTION

The fundamental knowledge of spray impingement is a key role to the advance of a large variety of technologies, such as those geared to improve combustion efficiency of internal combustion engines. In a spark ignition engine with port fuel injection (PFI), the fuel is injected onto the inlet port surface at the back of the intake valve. During cold starting, a film of liquid fuel forms at the inlet port, which is drawn into the cylinder during each intake stroke. This causes a fuel delivery delay and an associated inherent metering error due to only partial vaporization, thus making it necessary to supply amounts of fuel exceeding those required for the ideal mixture ratio. As a result, the engine experiences an unstable burn on the first 4 to 10 cycles of a cold start, with an associated significant increase in the emissions of unburned hydrocarbons. Moreover, technologic developments toward increasing engine efficiency consider shut down of the engine whenever the car is not moving. Again, PFI may raise difficulties to the demand of a smooth and fast restart. A more efficient control of the fuel supplied to the cylinder at cold start conditions can be achieved if the interaction between the gasoline spray and the time-varying liquid film which forms during the period of injection can be accurately predicted

Several works have been reported which consider the impact of either single droplets (e. g., Mundo *et al.*, 1995; Cossali *et al.*, 1997) or poly-dispersed sprays (e. g., Tropea and Roisman, 2000) but only a few consider the effects of a cross flow (e. g., Arcoumanis and Cutter, 1995; Panão and Moreira, 2003) or the presence of a liquid film at the target surface (e. g., Hardalupas *et al.*, 1993, Arcoumanis *et al*., 1997). In addition, it has been shown (Roisman et al., 1999 and Tropea and Roisman, 2000) that a poly-dispersed spray cannot be described by the superposition of several single droplet impact because other events, such as multiple drop impact with crown interaction (Roisman *et al.*, 2002, Tropea and Roisman, 2000 and Cossali *et al.*, 2003) and liquid film dynamics (Sivakumar and Tropea, 2002, Roisman and Tropea, 2002) also need to be modelled to accurately predict the outcome of spray impingement. Furthermore, in engine operation, fuel spray is transient due to pressure variations induced by pintle opening and closing, which further complicate the phenomena of liquid film formation and interaction. This feature further complicates the analysis of spray-wall-film interaction, which may vary during each injection period. The work reported here intends to contribute in that area.

The experiment consists of a multi-point injector spraying gasoline onto a flat disc located at 30mm. Measurements are made with a two-component PDA system in the near-wall region, which are processed in order to discriminate between droplets moving towards the wall and droplets moving out from the wall after interaction. The measurements are analysed based on conservation principles of mass, momentum and energy in order to infer about the interaction between the transient impacting spray and dynamics of the liquid film. The results provide new information to improve the accuracy of existing model tools available in the literature

2. EXPERIMENTAL SETUP AND DATA PROCESSING

2.1 Experimental Setup

The setup consists of pintle-type injector spraying into a flat aluminium disc 30 mm below the nozzle, with 0.4 μm of mean roughness and 36 mm in diameter. The injector produces a hollow-cone spray with interior and exterior spray angles of 8º and 19º, respectively. The fuel used in this experiment is commercial gasoline with density $\rho = 751.4\ kg/m^3$, dynamic viscosity $\mu = 5.194 \times 10^{-4}\ kg/m \cdot s$, refractive index of $m = 1.44$ and surface tension $\sigma = 19.4\ mN/m$.

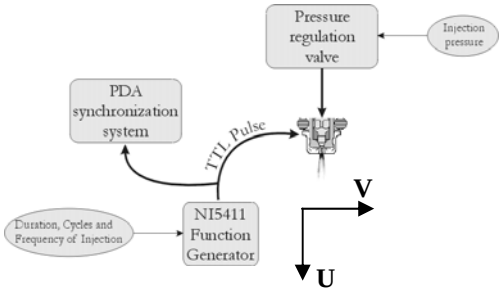

Fig. 1 Synchronism between the fuel injection and the PDA measurement system.

The time of injection and the time between successive injections, are controlled by an arbitrary function generator, NI5411, while the pressure of injection is manually controlled by a pressure regulation valve. Droplet sizes and velocities are measured with a two-component DANTEC phase Doppler system (PDA). The TTL signal used to trigger the fuel injector is the time reference for data synchronization and is used as a reset pulse for the PDA processor. Fig. 1 shows a scheme of the synchronization between fuel injection and PDA data acquisition. It is worth-mentioning that, despite the electromechanical delay between electronic opening and closing of the injector and fuel release (quantified as 1.6 ms and 1.3 ms, respectively), has not been taken into account for phase average processing.

The experiments reported here were obtained for operating conditions representative of a spark ignition engine at cold start. The target surface is kept at ambient temperature (20ºC) and a

liquid film forms upon spray impact. To avoid an excess of fuel on the surface, a series of 7 injection cycles is considered followed by a dead period of 10 s between series. Pulse duration is set at 5 ms, injection frequency at 10 Hz and pressure at 3 bar, which corresponds to a bulk volume of fuel of 12.5 mg *per* injection. Measurements were made at 2 mm above the disc surface at radial coordinates, measured from the axis of the injector, $r \in \{0, 0.5, 1, 2, 3, 4, 5, 6\}$. The axial (U) and radial (V) velocity components correspond to velocity components normal and parallel to the surface, respectively, as shown in Figure 1. The signal of the axial velocity is henceforth used to discriminate droplets inflowing towards the surface from secondary droplets generated by impingement mechanisms. More than 50,000 validated droplets were sampled at each measurement point to assure deviations from the cumulative drop size distribution smaller than 10% for each time bin considered in phase average analysis (Tate, 1982) and smaller than 10% for the PDA flux quantities (Saffman, 1987).

2.2 Data Processing

Validated droplets are processed in phase using a time windows of 0.5 ms. Data processing includes the arithmetic mean drop diameter (AMD), the ensemble average of the axial and radial velocity components (<U>, <V>), droplet direction (γ) and PDA flux measurements which were calculated using the algorithm developed by Roisman and Tropea (2001). All quantities are described in table 1.

Table 1 – Quantities used in the phase analysis

Quantity	*Expression*
<U>, <V>, AMD	Ensemble average: $\langle\beta\rangle(t) = \frac{1}{N(t)}\sum_{i=1}^{N(t)}\beta_i$
γ	$\gamma_i = \mathrm{atan}\left(\frac{V_i}{U_i}\right)$
PDA flux quantities	$\dot{B} = \frac{1}{\Delta t}\sum_{i=1}^{N_{sv}}\frac{\beta_i \cdot \cos(\gamma_i)}{A_\gamma(D_k,\gamma_k)}$

where β is an arbitrary quantity, which in the case of the PDA fluxes may be the number, mass, momentum and energy fluxes (kinetic and surface). N(t) is the sample size in the time window centred on t and $A_\gamma(D_k, \gamma_k)$ is the cross section area of the measurement volume, which is size and direction dependent (for more details see Roisman and Tropea, 2001).

3. RESULTS AND DISCUSSION

3.1 Effects of the target surface on spray structure

Figure 2 shows high speed photographs of the impinging spray obtained with a CCD camera at 1000 FPS (Panão and Moreira, 2002) during the injection period. A toroidal wall-jet vortex is formed at spray impact due to interaction of the spray front with the quiescent surrounding air, which expands in the radial direction and drags smaller and slower secondary droplets generated at impact. Figure 3 compares the main characteristics (droplet mean velocity and size) with those measured at the same distance from the nozzle, but without interposition of the target. These conditions are referred henceforth as the impinging spray and the free spray, respectively, and allow to infer about the effects of the target on the structure of the spray. The results show that the transient behaviour of the spray may be divided in three periods, as also reported by Panão and Moreira, 2004 and Abo-Serie et al., 2003: *i)* the *leading front of the spray* (LFS), characterized by large gradients of mean drop size and velocity; *ii)* the *steady spray* (SS), characterized by constant drop size and velocity and *iii)* the *spray tail* (ST), characterized by asymptotic decreases of drop size and velocity. Figure 3 further shows that the interposition of the disc does not induce any abrupt change in the qualitative distributions, although it induces a general increase of droplet mean size.

Leading front of the spray Steady spray End of steady spray Spray tail

Fig. 2 – Images of spray impingement during the injection period.

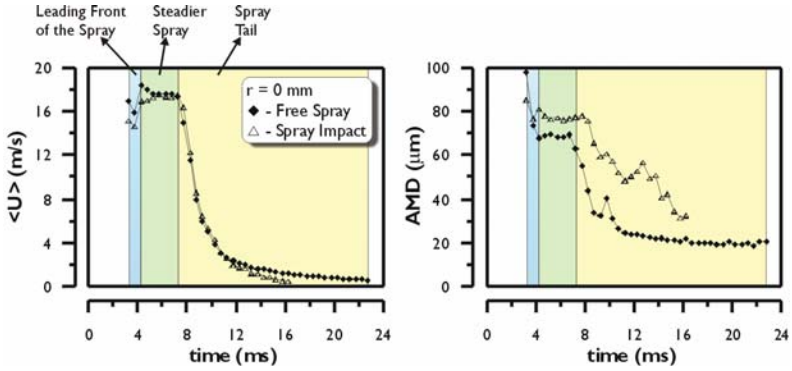

Fig. 3 – Mean droplet velocity and size during injection without (free spray) and with interposition of the disc.

The effects of impact on fluid-dynamic characteristics of the spray may be inferred from the direction of droplet velocity vectors. Figure 4 depicts the variation of the local angle of velocity vectors during the period of injection, estimated from time-resolved measurements of the two orthogonal velocity components, *U* and *V*, made at the same distance from the nozzle. The instantaneous value of droplet axial velocity is further used in Figure 4 to discriminate droplets moving towards the target (positive *U*) from droplets moving out from the target after impact (negative *U*).

In general, the results show that interposition of the disc alters the structure of the primary spray issuing from the nozzle and, therefore, the outcome of droplets after impact cannot be accurately predicted based on the characteristics of the spray, but requires precise knowledge of the flow structure induced by the target. The effects vary in magnitude during the period of injection and behave differently in the vicinity of the geometrical axis of the spray and in the outwards region. Inflowing droplets in the leading front and steady periods of the free spray (LFS and SS in Figures 2 and 3) are deviated outwards by the target surface (larger positive angle), while inflowing droplets in the tail of the impacting spray correspond to droplets entrained by the shear-induced vortex of air. Time dependence of droplet characteristics at impact in the vicinity of the stagnation region is caused by pressure variations induced by pintle-opening. Larger deviations occur at locations far from the geometrical axis of the spray, where droplets have smaller velocities and, therefore, are more sensitive to drag forces with the air flow induced by the presence of the disc. There, time variations of impact conditions are mainly associated with time growth of the three-dimensional vortical structure.

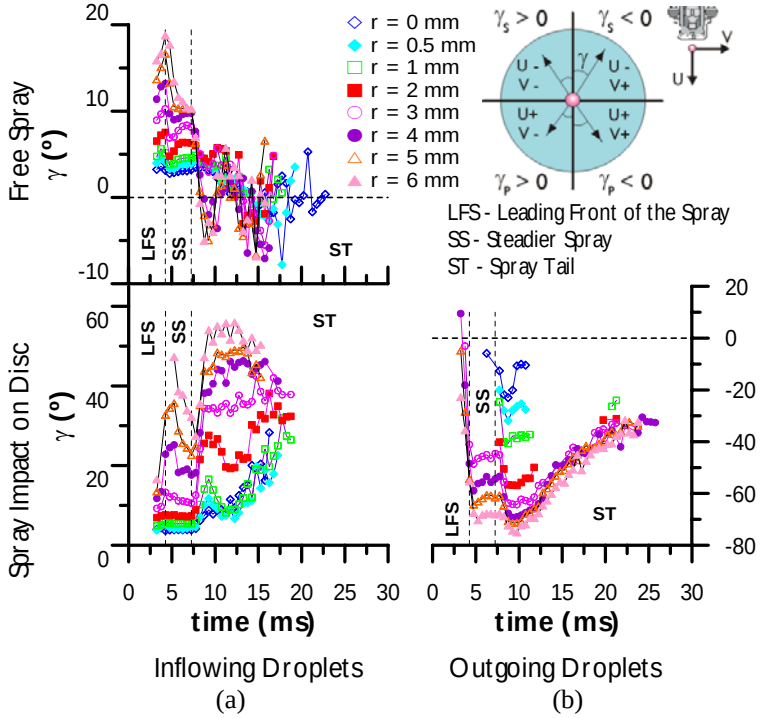

Fig. 4 – Time variation of droplet velocity vectors: (a) inflowing droplets in the free and impacting sprays; (b) outgoing droplets generated at impact.

The direction of droplets ejected from the surface depends on the angle of incident droplets but also on the mechanisms of interaction with the surface. In general, Figure 4b) shows that the impact increases the transverse momentum of droplets. This feature is either due to transfer of the normal momentum of inflowing droplets into the transverse component, as reported by Mundo *et al.* (1998), or to interaction with the time growing liquid film which rapidly spreads onto the surface, as suggested in Panão and Moreira, 2004.

The aim of the foregoing analysis is to account for the effects of the time dependent liquid film on the mechanisms of spray-wall interaction.

3.2 Evaluation of mass, momentum and energy fluxes transferred into the liquid film

In order to evaluate the amount of mass, momentum and energy transferred into the liquid film, a simple analysis is made here based on the application of conservation principles to each single droplet of the impinging polydispersion:

Mass:
$$m_i = \sum_{k=1}^{N_s} m_{s_k} + m_{LF} \tag{1}$$

Momentum:
$$\begin{aligned} m_i u_{ri} &= \sum_{k=1}^{N_s} m_{s_k} u_{rs_k} + p_{LF}^{U_r} \\ m_i u_{zi} &= \sum_{k=1}^{N_s} m_{s_k} u_{zs_k} + p_{LF}^{U_z} \end{aligned} \tag{2}$$

Energy:
$$\underbrace{\frac{1}{2} m_i u^2}_{E_{ki}} + \underbrace{\pi d_i^2 \sigma}_{E_{si}} = \underbrace{\frac{1}{2} \sum_{k=1}^{N_s} m_{s_k} u_{s_k}^2}_{E_{ks}} + \underbrace{\sum_{k=1}^{N_s} \pi d_{s_k}^2 \sigma}_{E_{ss}} + E_{LF} + E_{diss} \tag{3}$$

where $\mathbf{m_i}$ is the mass of an impinging droplet (subscript i), $\mathbf{m_s}$ is the mass of a secondary droplet (subscript s) and $\mathbf{m_{LF}}$ is the mass of the liquid film (subscript LF). The term **u** designates the velocity vector, **d** corresponds to drop diameter, $\mathbf{p_{LF}}$ the momentum transferred into the liquid film, $\mathbf{E_{k\ or\ s}}$ are the kinetic and surface energies, respectively, $\mathbf{E_{LF}}$ is the energy transferred into the liquid film and $\mathbf{E_{diss}}$ is the viscous dissipation energy estimated as in Mao *et al.* (1997), where the maximum spread diameter is computed from the model in Pasandideh-Fard *et al.* (1996).

Assuming that each impinging droplet originates N_s secondary droplets of the same size and velocity, the fractions (α) of mass, momentum and energy transferred into the wall-liquid film may be re-written in the following form:

$$\underbrace{\alpha_M = 1 - \frac{\sum_{k=1}^{N_s} m_{s_k}}{m_i}}_{\text{mass fraction}} \quad \underbrace{\alpha_{pUr} = 1 - \frac{\sum_{k=1}^{N_s} m_{s_k} u_{rs_k}}{m_i u_{ri}}}_{\text{radial momentum fraction}} \quad \underbrace{\alpha_{pUz} = 1 - \frac{\sum_{k=1}^{N_s} m_{s_k} u_{zs_k}}{m_i u_{zi}}}_{\text{axial momentum fraction}} \quad \underbrace{\alpha_e = 1 - \frac{E_{diss} + E_{ks} + E_{ss}}{E_{ki} + E_{si}}}_{\text{energy fraction}} \tag{4}$$

Therefore, if the fraction of an arbitrary property ($\theta \equiv$ mass, axial or radial momentum and energy) is defined as:

$$\alpha_\theta = 1 - \frac{\theta_{o\ (outgoing)}}{\theta_{i\ (inflowing)}} \tag{5}$$

four transfer modes may be identified as follows:

$$\begin{cases} \alpha_\theta = 1 \Rightarrow \text{Full transfer of } \theta_i \text{ to } \theta_{LF} & \text{Mode 1} \\ 0 < \alpha_\theta < 1 \Rightarrow \text{Partial transfer of } \theta_i \text{ to } \theta_{LF} & \text{Mode 2} \\ \alpha_\theta = 0 \Rightarrow \text{Full transfer of } \theta_i \text{ to } \theta_o & \text{Mode 3} \\ \alpha_\theta < 0 \Rightarrow \text{Partial transfer of } \theta_{LF} \text{ to } \theta_o & \text{Mode 4} \end{cases}$$

Figures 5-8 show the time variation of each fraction α_θ at several radial locations from the spray axis. The absence of points indicates an insufficient sample size of either inflowing, or outgoing droplets, to estimate statistically independent time averages.

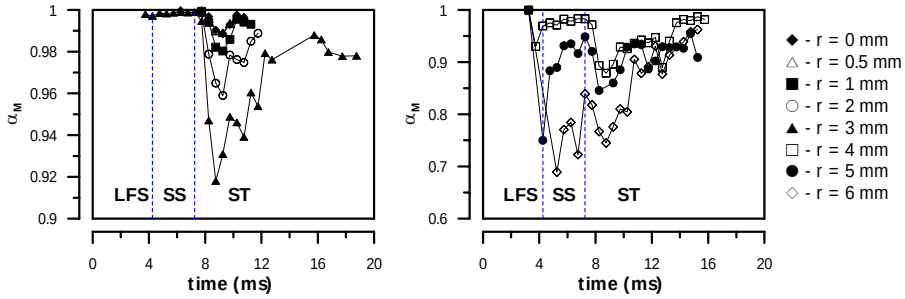

Fig. 5 – Time variation of the mass transfer coefficient (α_M)

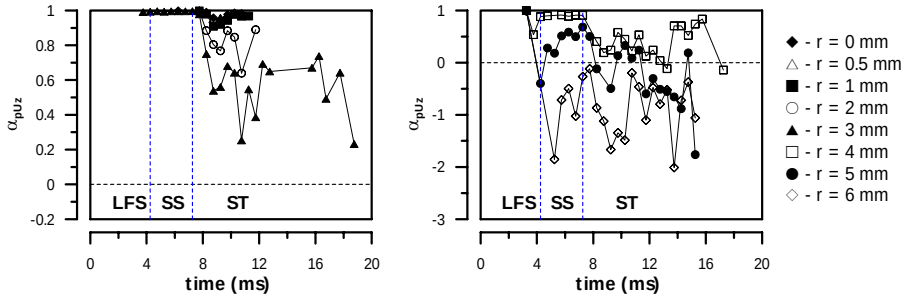

Fig. 6 – Time variation of the axial momentum transfer coefficient (α_{pUz})

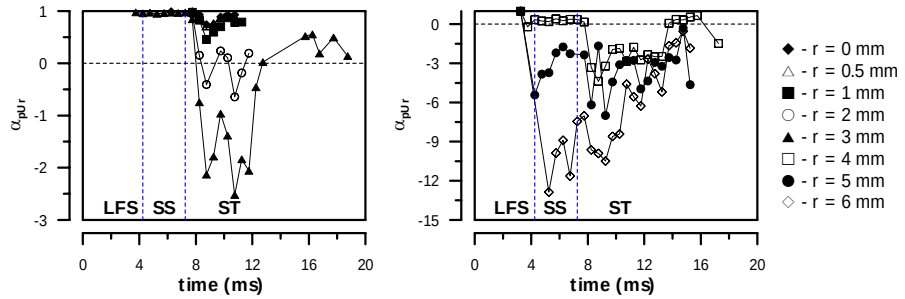

Fig. 7 – Time variation of the radial momentum transfer coefficient (α_{pUr})

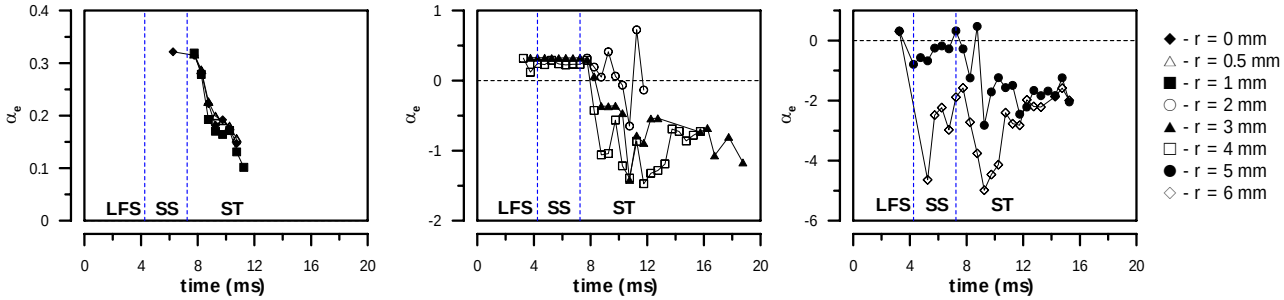

Fig. 8 – Time variation of the energy transfer coefficient (α_e)

The results show that all the mass and momentum impacting in the vicinity of the spray axis (r < 4 mm) during the leading (LFS) and steady (SS) periods are transferred into the liquid film (α_M, α_{Pu} = 1), but only part of the energy is transferred. Similar results have been also reported by Mundo *et al.* (1998) and show that the liquid film starts to form in the vicinity of the stagnation region at early stages of injection. At outer regions (r > 4 mm) a non-negligible part of droplets impinging during LFS and SS periods is ejected after having interacted with the wall by mechanisms of rebound and splash, as described in Panão and Moreira (2004).

The spray tail (ST) behaves differently, since transfer from the spray to the film is only partial. However, a peculiar feature is observed in the distributions of momentum transfer, α_{pu}: negative values denote that the liquid film contributes to the momentum of outgoing droplets (mode 4 of interaction), mainly in the direction parallel to the surface. This is associated with, both, re-atomization by film stripping and to fast radial movement of the liquid film induced by the impact at the stagnation region. Radial momentum is imparted to the liquid film by droplets sticking at the stagnation region, and feeds back onto secondary droplets at outwards locations, where momentum of impacting droplets is much smaller.

3.3 Influence of mass, momentum and energy fractions transferred to the liquid film in spray/wall interaction modelling

Most of spray/wall interaction models are based on experiments performed in steady-state conditions, for which the dynamic behaviour of the film is associated with the stochastic event of multiple drop impact. However, in our experiment, besides multiple drop impact of a poly-dispersed spray, also the transient behaviour during injection appears to be associated with dynamic changes of the liquid film. Only a few models reported in the literature to predict spray/wall interaction take into account the crown interaction for a multiple drop impact situation (Roisman and Tropea, 2000). In Sivakumar and Tropea (2001), besides crown interaction, also liquid film dynamics is suggested to be an important parameter that should be considered in the formulation of spray impact models. In Roisman and Tropea (2002) an attempt is made to model the flow on a wall surface due to spray impact. However, the spray is considered as a continuous in space, which, in the present case is only locally true and does not hold within the whole hollow-cone structure of the spray, as in typical port-fuel injection systems. The objective of the analysis performed herein is to follow the approach of Roisman and Tropea (2000) and to suggest improvements for modelling spray/wall interaction making use of the transfer coefficients α_θ described before. The original model predicts the mass flux ratio based on the use of two parameters:

1. a parameter characterizing crown interaction (λ) defined for the phase Doppler technique as:

$$\lambda = \frac{29.75}{\Delta t}\sum_{i=1}^{N_{sv}} \frac{\eta_{vi} D_i^4 u_{zi}^2}{A_{\gamma i}\left(D_i,\gamma_i\right)} \frac{\cos\left(\gamma_i\right)\rho\mu}{\sigma^2} \tag{6}$$

where Δt is the time window times the number of pulses; N_{sv} is the sample size in each time bin; η_v is a correction factor for multiple scattering inside the detection volume, which was set to one in the present case; D_i, γ_i and u_{zi} are the size, direction and axial velocity of each validated drop; $A_{\gamma i}$ is the effective area of the detection volume; and ρ,μ ,and σ are the density, viscosity and surface tension of the liquid.

2. a predicted mass flux ratio, η_{m0}, as the ratio between the mass predicted after impact (m_{a0}) and the mass of impacting drops (m_b). The term m_{a0} is approximated to the superposition of single drop impact and is estimated as the summation of each impacting drop mass times an empirical correction factor (η) calculated for the i^{th} drop as

$$\eta_i = 1.2\left\{1 - \frac{1}{1+\exp\left[\left(K_i - 2823.6\right)/357.7\right]}\right\},\ K_i = \left(We_i\sqrt{Re_i}\right)^{4/5} \tag{7}$$

Although the authors consider the presence of a liquid film at spray impact, no information is given about the range of film thickness for η_i to be valid, which can be a source of discrepancies with the experimental results. However, since the implications of this for the present analysis are not easy to formulate with the information available, it is considered as a limitation of the model from this point on.

The mass flux ratio predicted by the original model (Roisman and Tropea, 2000) is then expressed as

$$\eta_m\left(\mathrm{model}\right) = \eta_{m0}\left(1 + 0.43\eta_{m0}^{-0.2}\lambda^{0.023}\right),\ \eta_{m0} = m_{a0}/m_b \tag{8}$$

The PDA measurements are used to compute experimental values of flux ratios between the secondary and inflowing droplets for number (η_n), mass (η_m), momentum (η_p) and energy (kinetic and surface - η_e). Fig 9(a) compares the predicted mass flux ratios with the corresponding experimental values along the period of spray impact. The Figure shows that part of the experimental results is over-predicted by the model, while the remaining is under-predicted.

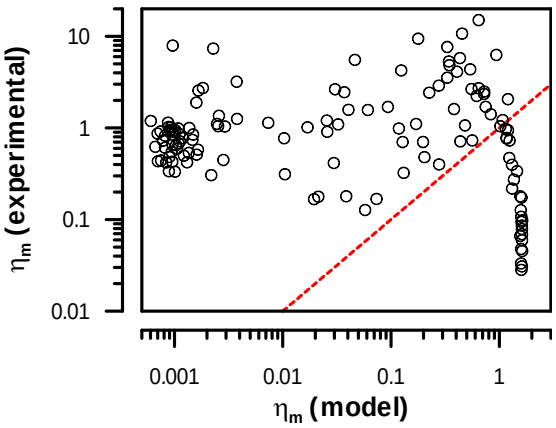

Fig. 9 -. Comparison of mass flux ratios obtained from PDA measurements with those computed as in Roisman and Tropea (2000).

Careful analysis shows that over-predicted values correspond to those for which the mass transfer coefficient in Fig. 5 is close to unity (α_M = 1), while under-predicted values correspond to those for which $0 < \alpha_M < 1$. This observation clearly suggests that discrepancies between experiments and predictions may be attributed to the interaction of the poly-dispersed spray with the impacted transient liquid film: the model is not able to account for the deposited mass in the region where $\alpha_M = 1$, neither is not able to account for the possible increase of the size of secondary droplets when the spray impacts onto a liquid film where $0 < \alpha_M < 1$ (*e.g.*, Mundo *et al* 1998). An attempt is made here to account for the effect of the liquid film based on the transfer coefficients analysed in Fig. 5.

For that, the transfer coefficients are expressed in the form $(1 - \alpha_\theta)$ and introduced as parameters in the empirical correlations. The resulting new correlations are described in Table 2. There, the flux ratio of energy accounts for both, surface and kinetic energy, while the original empirical correlations suggested by Roisman and Tropea (2000) consider separated contributions.

Table 2 – Empirical correlations for spray/wall interaction modelling

Flux Ratio	*Roisman and Tropea*	*New correlation as function of $(1 - \alpha_\theta)$*
Number	$\eta_n = 2.69 \cdot \eta_m^{1.4}$	$\eta_n(\alpha_\theta) = 0.822 \cdot \eta_m^{1.361} \cdot (1-\alpha_M)^{-0.221} \cdot (1-\alpha_{pUz})^{0.084} \cdot (1-\alpha_{pUr})^{-0.483} \cdot (1-\alpha_e)^{0.219}$
Momentum	$\eta_p = 0.29 \cdot \eta_m^{1.19}$	$\eta_p(\alpha_\theta) = 0.279 \cdot \eta_m^{0.708} \cdot (1-\alpha_M)^{-0.398} \cdot (1-\alpha_{pUz})^{0.799} \cdot (1-\alpha_{pUr})^{-0.148} \cdot (1-\alpha_e)^{-0.043}$
Energy	$\eta_s = 1.29 \cdot \eta_m^{1.01}$ (surface) $\eta_k = 0.36 \cdot \eta_m^{1.11}$ (kinetic)	$\eta_e(\alpha_\theta) = 0.295 \cdot \eta_m^{0.484} \cdot (1-\alpha_M)^{-0.323} \cdot (1-\alpha_{pUz})^{0.705} \cdot (1-\alpha_{pUr})^{0.256} \cdot (1-\alpha_e)^{0.057}$ (total)

Fig. 10 depicts flux ratios predicted by the original and the improved models, versus the experimental values. The dotted line represents complete concordance. The results show that improvements may be achieved if the fractions α_θ are considered and their inclusion in spray/wall interaction models is suggested as a simple way of accounting for the influence of the liquid film. It is worth mentioning at this point that extrapolation of this analysis must be done with care, since it is based on a sole experimental condition. However, the purpose here is to evaluate the influence of the liquid film in the prediction of impact and not to suggest an alternative model to the existing spray/wall interaction approach.

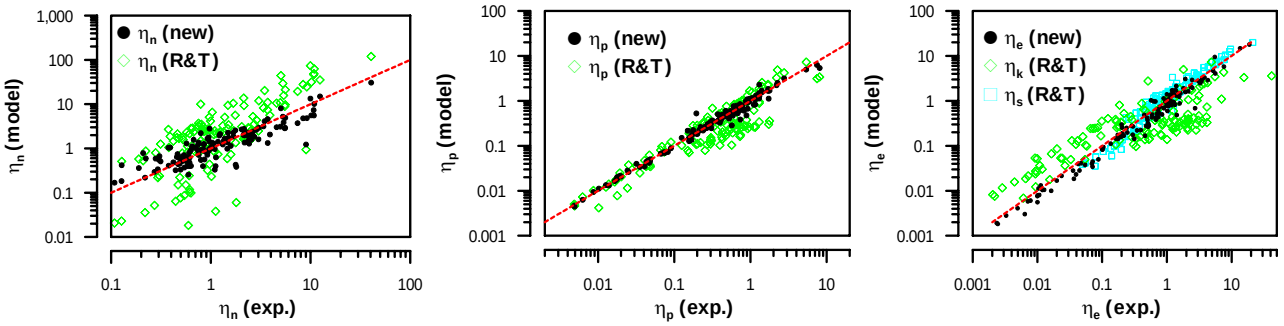

Fig. 10 –Plots comparing the number, momentum and energy flux ratios estimated with the original and modified empirical correlations and the experimental results.

4. SUMMARY AND CONCLUDING REMARKS

This paper considers part of an experimental study of spray-wall impingement aimed at contributing to optimize gasoline injection systems at cold start conditions. The experimental flow consists of a pulsed gasoline spray impinging onto a flat disc at ambient temperature, thus originating the formation of a time growing liquid film. A shear induced toroidal vortex forms at the surface, which grows during the injection period and entrains secondary droplets generated by splash, rebound and/or film stripping to re-impinge. A detailed characterization of the two-phase flow in the vicinity of the target wall is performed with a two-component PDA system. The results show that interposition of the disc alters the structure of the primary spray issuing from the nozzle and, therefore, the outcome of droplets after impact cannot be accurately predicted based on the characteristics of the spray, but requires precise knowledge of the flow structure induced by the target.

Time dependence of droplet characteristics at impact in the vicinity of the stagnation region is caused by pressure variations induced by pintle-opening. Larger deviations occur at locations far from the geometrical axis of the spray, where droplets have smaller velocities and, therefore, are more sensitive to drag forces with the air flow induced by the presence of the disc. There, time variations of impact conditions are mainly associated with time growth of the three-dimensional vortical structure.

The liquid film is mainly formed by droplets impinging within the stagnation region. Rapid radial expansion of the film caused by continuous feeding enhances the transfer of normal impact momentum into radial momentum which then feeds back onto secondary droplets at outwards locations, where momentum of impacting droplets is much smaller.

A simple analysis based on conservation principles, is performed to deepen knowledge of the influence of liquid film dynamics in the outcome of spray impingement. For that transfer coefficients are estimated to account for mass, momentum and energy transferred into the liquid film. These coefficients are further correlated with the mass flux ratio between outgoing and inflowing droplets to empirically express the number, momentum and energy flux ratios. Significant improvements may be achieved if these terms are included in spray/wall interaction models.

Acknowledgments

The authors acknowledge the contribution of the National Foundation of Science and Technology of the Ministry for Science and Technology by supporting M. R. Panão with a Research Grant through the project POCTI/ 1999/ EME/ 38082.

REFERENCES

Abo-Serie, E., Gavaises, M., Arcoumanis, C. (2003), “Spray/wall interaction in direct injection spark ignition equipped with multi-hole injectors”, Proceedings of the 9th Int. Conf. Liquid Atom. and Spray Systems (ICLASS), Sorrento.

Arcoumanis, C. and Cutter, P. A. (1995), “Flow and Heat Transfer Characteristics of Impinging Diesel Sprays Under Cross-Flow Conditions”, SAE Technical Paper 950448.

Arcoumanis, C., Whitelaw, D.S. and Whitelaw, J.H. (1997), “Gasoline injection against surfaces and films”, Atomization and Sprays, 7, pp. 437-456.

Cossali GE, Coghe A and Marengo M (1997), “The impact of a single drop on a wetted surface”, Exp. Fluids, 22, pp. 463-472

Cossali, G.E., Marengo, M., Santini, M., (2003), “Multiple drop impact on heated surface”, Proceedings of the 9th Int. Conf. Liquid Atom. and Spray Systems (ICLASS), Sorrento.

Hardalupas Y, Okamoto S, Taylor A M K P, Whitelaw J H (1992) “Application of a Phase Doppler Anemometer to a Spray Impinging on a Disc”, Adrian, Durão, Durst, Heitor and Maeda, Laser Tech and Appl in Fluid Mech, Proceedings of the 6th Int Symp, Lisbon, Portugal, pp. 490-506

Mao, T., Khun, D., Tran, H. (1997), "Spread and rebound of liquid droplets upon impact on flat surfaces", AIChE Journal, 43 (9), pp. 2169-2179.

Mundo C, Sommerfeld M and Tropea C (1995) "Droplet-Wall Collisions: Experimental Studies of the Deformation and Breakup Process", Int J Multiphase Flow, 21, pp. 81-173

Mundo C, Sommerfeld M and Tropea C (1998) "On the modelling of Liquid Sprays Impinging on Surfaces", Atomization and Sprays, 8, pp. 625-652

Panão MRO and Moreira ALN (2003) "Experimental characterization of intermittent gasoline sprays impinging under cross-flow conditions", to appear Atomization and Sprays.

Panão, M.R. and Moreira, A.L.N. (2002) "Visualization and Analysis of Spray Impingement under Cross-Flow Conditions", SAE Technical Paper 2002-01-2664.

Panão, M.R.O. and Moreira, A.L.N. (2004), "Experimental study of the flow regimes resulting from the impact of an intermittent gasoline spray", to appear in Experiments in Fluids.

Pasandideh-Fard, M., Qiao, Y., Chandra, S., Mostaghimi, J. (1996), "Capillary effects during droplet impact on a solid surface", Physics of Fluids, 8 (3), pp. 650-659

Roisman IV and Tropea C (2002) "Flow on a wall surface due to spray impact", Proceedings of the 18th Annual Conf on Liquid Atom and Spray Systems, Zaragoza.

Roisman IV, Araneo L, Marengo M and Tropea C (1999) "Evaluation of drop impingement models: Experimental and numerical analysis of a spray impact", Proceedings of the 15th Annual Conference on Atomization and Spray Systems, Toulouse.

Roisman, I.V. and Tropea, C. (2001), "Flux measurements in sprays using phase Doppler techniques", Atomization and Sprays, 11, pp. 667-700.

Roisman, I.V., Prunet-Foch, B., Tropea, C., Vignes-Adler, M. (2002), "Multiple drop impact on dry solid substract", J. Colloid and Interface Science, 256, pp. 396-410.

Saffman, M (1987), "Automatic calibration of LDA measurement volume size", Applied Optics, 26, pp. 2592-2597.

Sivakumar D and Tropea C (2002) "Splashing impact of a spray onto a liquid film", Physics of Fluids, 14 (12), pp. L85-L88.

Tate, R.W. (1982), "Some problems associated with the accurate representation of droplet size distributions", Proceedings of the 2nd Int. Conf. Liquid Atom. And Spray Systems, Madison.

Tropea C and Roisman IV (2000) "Modeling of spray impact on solid surfaces", Atomization and Sprays, 10, pp. 387 – 408.